

WP3 - Optimization

WP3 of the AirToHeat project included the research part of the project. The work package included scientific research on the evaporator design and layout as well as the development of simulation models for investigation of optimal control strategies for defrosting of large-scale ambient air source heat pumps (HPs).

The research part of the project was led by DTU Construct and carried out in close collaboration with the Danish Technological Institute (DTI) and the industrial partners. The research was carried out by one Postdoc and one Researcher at DTU Construct, who were both supervised by Associate Professor Wiebke Brix Markussen also from DTU Construct. At the Danish Technological Institute, researchers at the Center for Refrigeration and Heat Pump Technology contributed to the research work in close collaboration with LUVÉ and the other industrial partners.

Part of the research work summarized in this report was disseminated in a paper by Rogié et al. [1] and furthermore presented at the 7th International Symposium on Advances in Refrigeration and Heat Pump Technology. Additionally, one more paper is planned for publication. The research work furthermore formed the basis of the Master's Thesis of Matteo Daminato [2].

The objective of the research was to identify evaporator designs, evaporator layouts and defrost control strategies for large-scale ambient air source HPs, which can improve the energy efficiency of the HP significantly, by counteracting unwanted frost formation and unwanted cold air recirculation. The research objective was primarily investigated with numerical modelling and simulation.

The work in WP3 was divided into two research tasks:

- Task 1: Optimizing evaporator geometry and evaporator operation
- Task 2: CFD analysis of evaporator layouts and air recirculation

Both research tasks focused on case studies related to the evaporators of the district heating heat pump located in Brødstrup.

Case study: The Brødstrup heat pump

Brødstrup Fjernvarme established a 5.5 MW air source heat pump for production of district heating in 2020/2021. The heat pump is a two-stage ammonia heat pump with screw compressors on the low pressure stage and a reciprocating compressor on the high pressure stage. The ammonia evaporator consists of 20 evaporator units with eight fans on each unit. The units are clustered two by two and placed next to each other as indicated in Figure 1, showing the outline of the heat pump. The direction of the airflow is downwards through the heat exchanger.

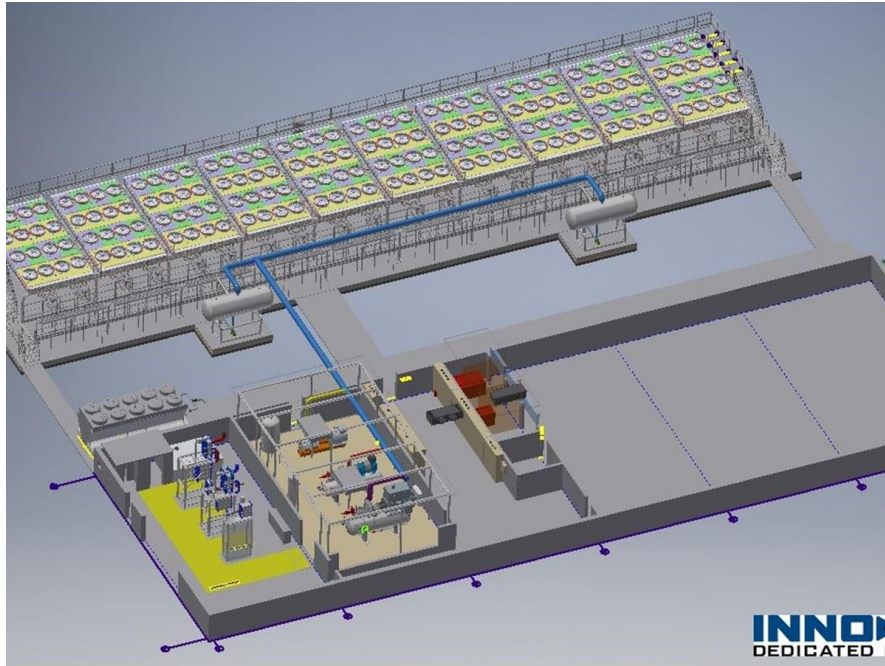


Figure 1: Sketch of the heat pump in Brædstrup. (Picture from www.braedstrup-fjernvarme.dk)

Task 1: Optimizing evaporator geometry and evaporator operation

The aim of this research task was, by means of numerical modelling, to investigate the influence of frost formation and frost build-up on the performance of the evaporators. An existing evaporator model [3], [4] was adapted for this purpose. The model was verified by comparison with LUVES calculation software and validated with measurements from the Brødstrup heat pump.

Methods

The evaporator model

The evaporator model was based on a model presented in [3] and [4]. The model is a discretized evaporator model with possibility of defining the refrigerant circuitry either in an inline configuration or in a staggered tube configuration as shown in Figure 2. The model solves energy and mass balances as well as the heat transfer equation using the epsilon-NTU method for each defined control volume. The model can further solve the refrigerant flow distribution between the individual passes of the refrigerant circuitry. This is done by solving the refrigerant mass flow rate through each pass such that pressure drops over each pass are equal.

Empirical correlations were used in order to calculate the convective heat transfer coefficients, void fraction and frictional pressure drop. Table 1 shows a summary of the correlations that were used for the present study. The model was implemented in Matlab [5] using thermodynamic and thermophysical properties from RefProp [6].

Table 1: Empirical correlations used in the evaporator model.

Air	Heat transfer coefficient	[7]
	Pressure drop	[8]
Refrigerant, single phase	Heat transfer coefficient	[9]
	Tube friction	[10]
	Bend friction	[11]
Refrigerant, two-phase	Heat transfer coefficient	[12]
	Tube friction	[13]
	Bend friction	[14]
	Void fraction	[15]

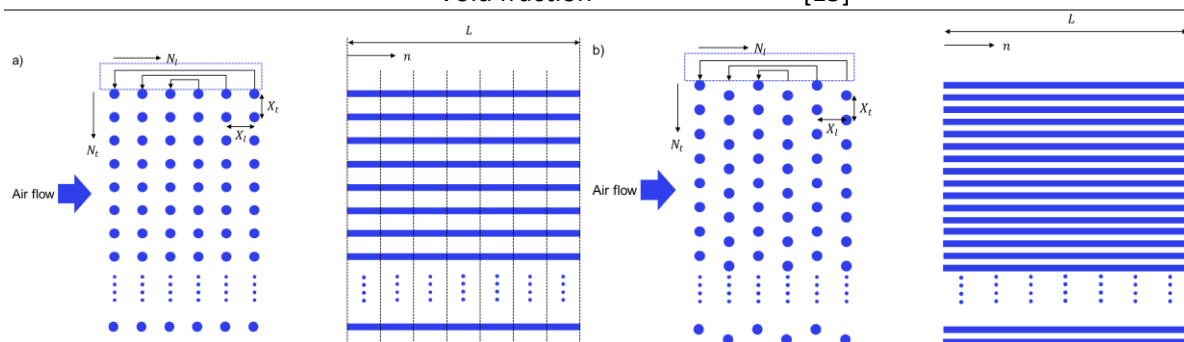


Figure 2: a) Inline arrangement of refrigerant tubes, front view and side view. b) Staggered arrangement of the refrigerant tubes, front view and side view.

Non-uniform airflow distribution

For an evaporator, where the air is blown through by the fans the air velocity beneath the fan area will be higher than the air velocity at the edges of the coil due to a pressure gradient over the top of the coil. The evaporator model was adapted to include the possibility for adapting the pressure

gradient above the coil, such that a 1-dimensional non-uniform velocity profile through the coil was generated as illustrated in Figure 3.

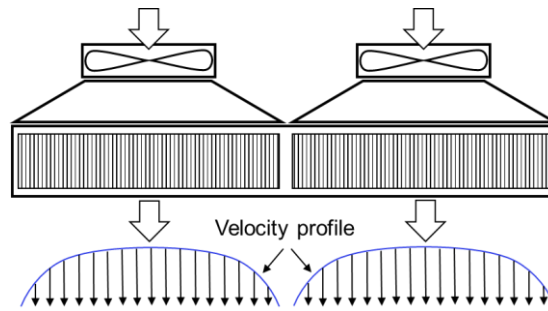


Figure 3: Velocity profile of air flow resulting from a non-uniform pressure gradient over the coil.

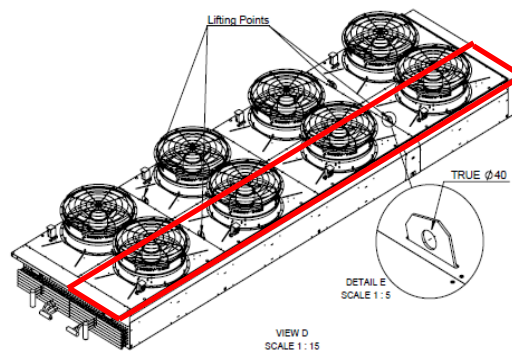


Figure 4: Illustration of one evaporator unit with eight fans. The refrigerant enters the coil through two inlet manifolds. Figure from XX

Due to the symmetric arrangement of the refrigerant tubes into the coils seen in Figure 4 it was possible to reduce the calculations to $\frac{1}{4}$ of the evaporator. A pressure gradient was applied along the parallel refrigerant tubes, as shown in Figure 5, and based on a requirement of uniform pressure at the outlet of the coil, the velocity distribution was calculated.

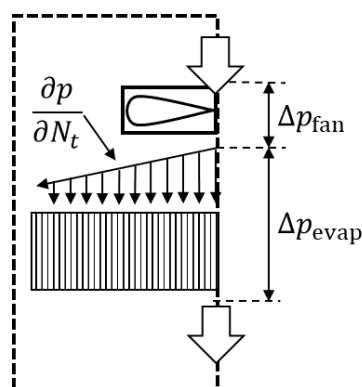


Figure 5: A pressure distribution above the coil was used to calculate the air velocity distribution.

Fan characteristics

In order to couple the fan characteristics and thus the volume flow rate of air through the evaporator coil to the pressure drop through the coil, a fan characteristic was added to the evaporator model. Figure 6 shows the fan characteristic, which was created based on the fan characteristic provided in the datasheet of the fan used in the evaporator units. For a given fan speed the black solid curves

show the relation between the pressure difference over the fan and the volume flow rate of air, that the fan will move. The dashed curves show the same relation for regions out of the intended operating range. As the pressure above the fan is equal to the pressure below the coil, the pressure increase through the fan equals the pressure drop through the coil. For fan speeds in between the curves shown in Figure 6 an interpolation was made.

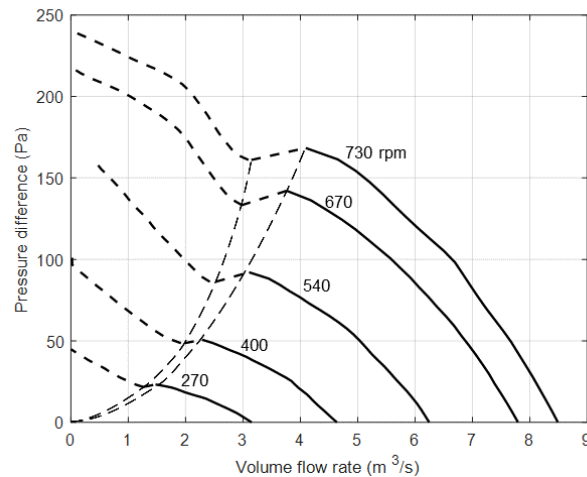


Figure 6: Fan characteristic used in the evaporator model.

Frost formation and accumulation

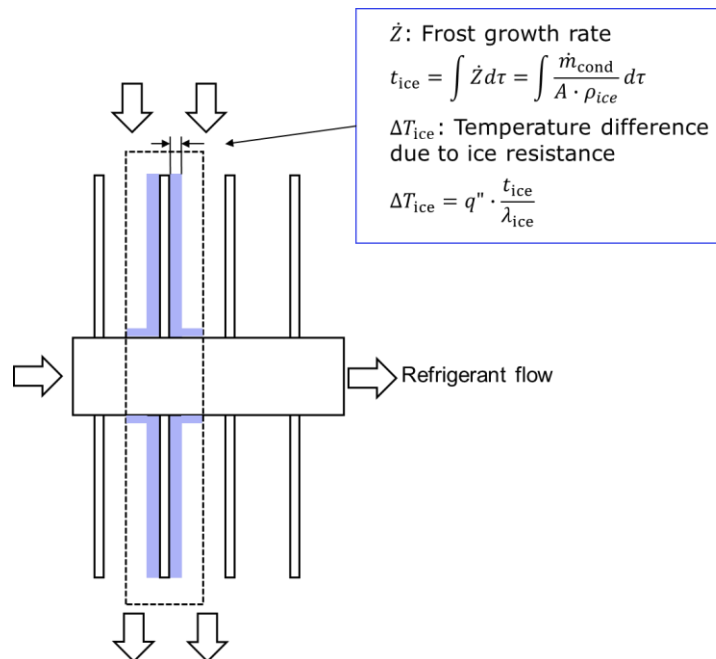


Figure 7: Principle sketch of frost build-up on the fin surface

Figure 7 depicts how frost is accumulated on the finned surface. The mass transfer of water onto the evaporator surface is calculated as described in [3]. In the present model, it was assumed that when the fin surface temperature was below 0 °C all the mass transfer of water to the surface accumulates as frost on the surface. By accounting for the fin area and the frost density the frost growth rate can be determined. The accumulation of frost was subsequently determined as the integral of the frost growth rate.

The effect of the accumulated frost on the performance of the evaporator was accounted for by two contributions: increased thermal resistance and increased flow resistance. The increased thermal resistance depends on the frost thickness and the frost conductivity while the increased flow resistance depends only on the frost thickness. The frost thickness reduces the free flow area for the air flow through the evaporator. When combined with the fan characteristics this results in a reduction of mass flow through the evaporator as frost accumulates on the surface.

De-frost modelling

Defrost is assumed to be hot gas defrost using hot gas from the open intercooler at the intermediate pressure. The models assumed a fixed defrost time of 15 minutes and subsequently the hot gas consumption is determined by an energy balance, calculating first the average heat flow needed to melt the accumulated frost in 15 minutes and subsequently the mass flow gas that should be condensed to deliver this heat flow.

Evaporator operation

The operation of the entire evaporator field with frost accumulation and defrost was also modelled. The model takes as input, the number of evaporators units in the system as well as the defrost time. This is given as matrix indicating a which point in time each individual evaporators are defrosted.

For the Brædstrup heat pump 20 evaporator units are installed and the units are defrosted in pairs of two at a fixed time interval. Thus, at any point in time during operation all evaporator units will be in different states of frost accumulation and further two units may be out of operation due to defrost. As all units are connected to the same compressor, they operate at a common evaporator pressure and thus common temperature. However, as the performance of the evaporators are affected by their state of frost accumulation the units do not deliver an equal distribution of the total evaporator load.

It was assumed that both the low pressure and high pressure compressors were speed controlled to ensure the delivered heat load and the intermediate pressure, respectively. Hence, the model can determine the evaporating temperature by ensuring that the total mass flow of vapour delivered by the sum of all evaporators is maintained. This includes both the mass of vapour needed to maintain the heat load plus the mass flow of vapour needed for hot gas defrost of the evaporators.

This assumption is valid for small variations in evaporation and ambient temperature as it implicitly assumes a constant COP of the heat. The assumption was applied for simplicity as this subsequently only requires the evaporators to be modelled. For larger variations in evaporation or ambient temperature or for alternative compressor speed control strategies a complete heat pump system model should be applied to attain reliable results.

Model validation

The results of the developed model was verified by comparing the simulations to the data sheet of the evaporator units installed in Brædstrup. Further, the model results have been compared with the measured data from the evaporators installed in Brædstrup.

Table 2 presents the verification with the evaporator data sheet supplied by LuVe. It should be noted that data in the data sheet are results from of LuVe's calculation tool and not measured data. However, LuVe's calculation tool has been validated against measured data from evaporators installed in their laboratory. LuVe's calculation tool did not account for the latent heat of fusion from the frost formation. Hence, for the results that are affected by this, the results from the developed model are shown both with and without this contribution.

As seen in Table 2, the developed model generally shows a good agreement with the validated results from LuVe's calculation tool. The largest deviation was on the pressure drop on the refrigerant side where the developed model underestimates by 19 %. The remaining results are within the acceptable tolerances for such a model.

Table 2: Comparison of the developed model and the LuVe calculation tool

	LuVe	DTU	Deviation
\dot{m}_{ref}	0.301 kg/s	0.301 kg/s	0 % (input)
CR	2	2	0 % (input)
\dot{Q}	195.7 kW	195.0 kW	0.35 %
SHR	0.750	0.733 (0.754 without latent heat of fusion)	2.5 % (0.5 %)
T_{evap}	-10.6 °C	-9.70 °C	0.9 °C
$T_{\text{air,o}}$	-7.97 °C	-7.95 °C	0.05 °C
Δp_{ref}	0.70 kPa	0.57 kPa	19 %
Δp_{air}	20.9 Pa	20.2 Pa	5.0 %
\dot{V}_{air}	100,000 m ³ /h	101,211 m ³ /h	1.2 %
\dot{m}_{cond}	72 kg/h	67 kg/h (75 kg/h without latent heat of fusion)	7.0 % (4.2 %)
$x_{\text{air,o}}$	1.88 g/kg	1.91 g/kg (1,87 kg/h without latent heat of fusion)	3.0 % (0.5%)

In addition to the comparison with LuVe's calculation tool the results of the model have been compared to the measurements collected from the evaporators installed in Brædstrup. This comparison may be seen in Table 3. As seen, there is a significant disagreement between the measured and simulated data. However, validation was difficult due to several issues. As the evaporators were flooded no reliable measurement of the heat load on the individual evaporator units were performed. Therefore, the total evaporator load had to be estimated from an energy balance of the entire system. However, measurements were only performed on two out of 20 units and thus, the accumulated frost or defrosting of other units means that the total load cannot be distributed to the individual unit as a simple average.

In conclusion, the deviations between the measurements and simulations are apparent but may stem both from improper estimation of the boundary conditions and from inconsistencies between the modelled and actual physics. More data would be needed to distinguish between these two contributions.

Table 3: Comparison of the developed model with the measured data from Brædstrup

	Brædstrup data	DTU model	Deviation
T_{evap}	-7.8 °C	2.60 °C	10.4 °C
$T_{\text{air,o}}$	1.4 °C	3.92 °C	2.52 °C
Δp_{ref}	0.165 kPa	0.18 kPa	8 %
Δp_{air}	15.9 Pa	20.7 Pa	25%
$x_{\text{air,o}}$	4.1 g/kg	5.0 g/kg	22 %

Results

Model simplification

Although the model is capable of calculating the local frost accumulation and the subsequent induced refrigerant and air misdistribution, it was found that the spatially distribution of these phenomenon had minor influence on the overall results on the evaporator performance under the influence of frost accumulation.

Figure 8 presents a comparison of the simulated results when making the full calculation on all 44 pipe rows and accounting for refrigerant and air misdistribution to a simplified model formulation with only one pipe row and an imposed equal distribution of air and refrigerant. As seen in Figure 8 this simplification results in a minor error on the air side pressure drop and consequently the fan power as well as a minor error on the evaporation temperature.

As the deviation between the detailed and simple model was found to be insignificant and the simplified model results were significantly less computationally demanding, the subsequent analysis were performed using simulations of the simplified model.

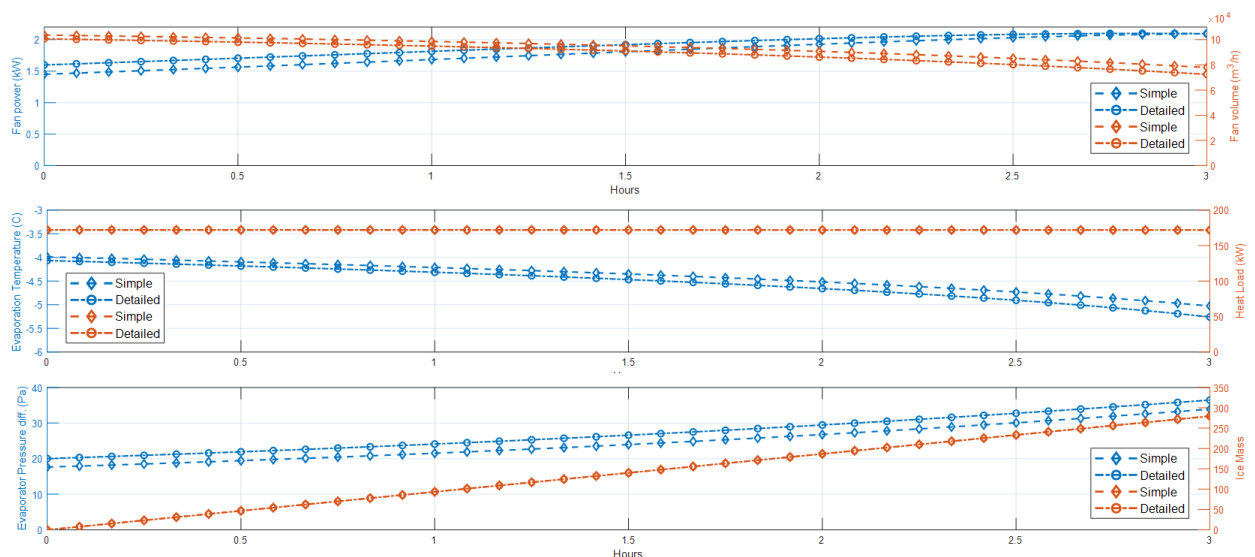


Figure 8 Comparison of detailed and simplified model.

Fixed speed vs fixed volume

Figure 9 and 10 shows how the evaporator performance was influenced by frost formation under fixed fan speed operation and under variable speed operation where the fan speed was increased to ensure a constant volume flow rate of air. It should be noted that this simulation was for 1 row out of 44 and thus all values besides pressure drop should be scaled by 44 to represent the full evaporator unit.

It may be seen that after 5 hours of operation the ice thickness for the two fan control strategies are comparable and has increased to approximately 1.2 mm. However, it may also be seen that the effect on the heat load and fan power are significantly different. With fixed fan speed the heat load is reduced by approximately 20 % while the heat load reduction for constant air flow is only approximately 2 %. Conversely, the fan power consumption increases to approximately 6 W for constant speed but up to 14 W for constant flow rate.

This trend was caused by the fact that the main contribution to the reduction of heat transfer performance when frost was formed was the hydraulic effect. Hence, the reduced air velocity caused

by the fan characteristics. While the increased thermal resistance induced by the layer of frost was only a minor contribution.

In conclusion, the heat load of the evaporators can be maintained under frosted conditions if the fan speed can be increased to attain the same air flow rate with the increase flow resistance. However, this does infer a significant increase in fan power, which should be compared to the reduced power consumption of the compressors attained by the higher evaporation temperature.

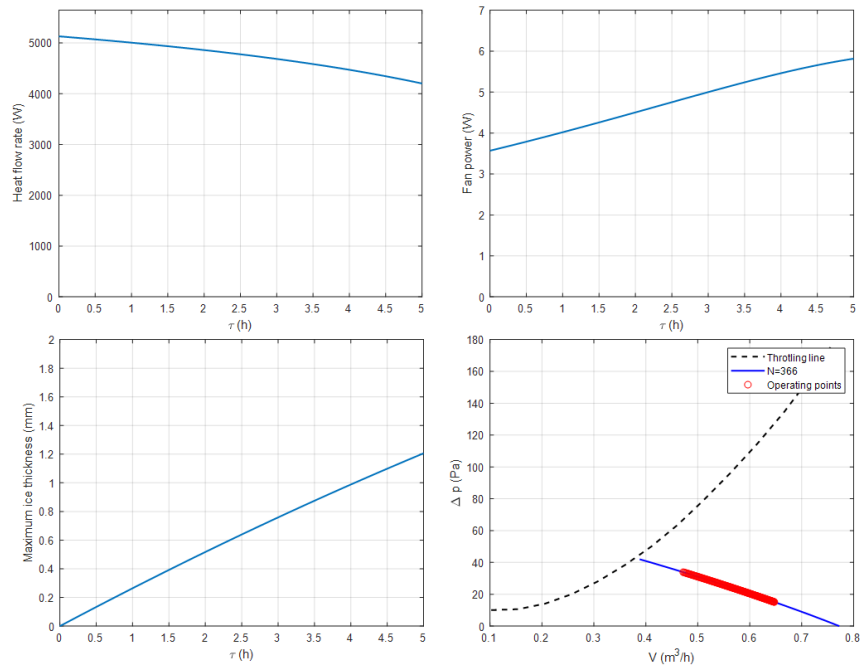


Figure 9. Changes in heat load, Fan power, Ice thickness, and air side pressure drop and volume flow rate after 5 hours of frost formation as constant evaporation temperature and constant fan speed

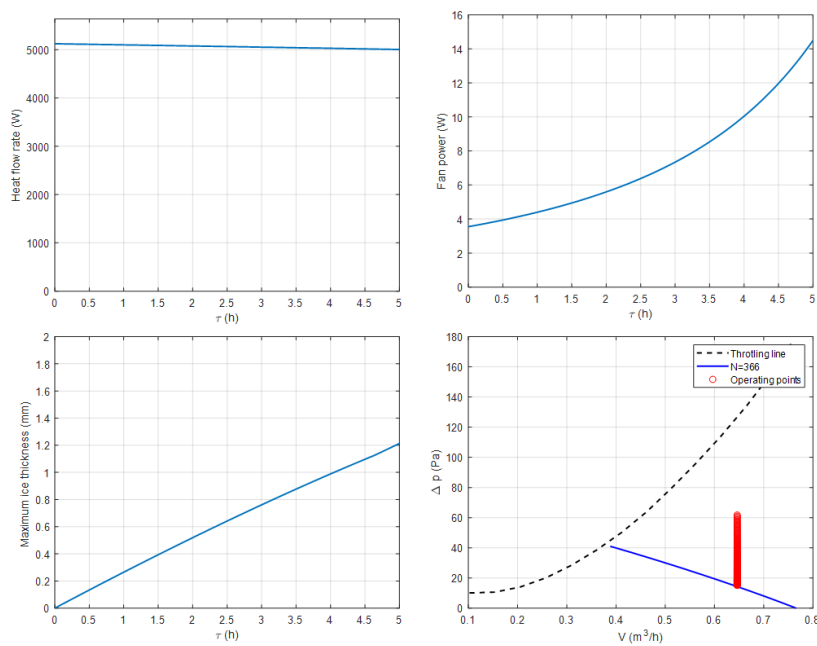


Figure 10 Changes in heat load, Fan power, Ice thickness, and air side pressure drop and volume flow rate after 5 hours of frost formation as constant evaporation temperature and variable fan speed to ensure constant air volume flow rate

Evaporator field operation

Figure 11 shows a simulation of the entire evaporator field in Bræstrup. The simulation was performed for an eight-hour period in which the evaporators were defrosted every 3rd hour. The simulations were initiated with all 20 evaporators free from frost and with the initiation of a defrost sequence the evaporators were defrosted one at a time for 15 minutes. This means that little frost was removed in the first defrost. However, as seen on Figure 11 the accumulated ice mass seemingly attains a cyclic behavior already after the second defrost.

It may be seen from Figure 11 that although the average heat load (red line) was maintained, the distribution of the heat load between the units was significant, varying from approximately 160 kW to 200 kW depending on the individual units' state of frost accumulation. Equally, it may be seen that the fan power is highly influenced by the amount of accumulated frost. As seen, the fan power was around 35 kW per unit when no ice has been formed and peaks at approximately 44 kW when the amount of accumulated frost peaks.

Further, Figure 11 clearly shows the evaporation temperature was also affected by the accumulated frost as well as on the amount of units that are out of operation due to defrost. Around hour 3 and 6 a clear drop in evaporation temperature is observed. This, as one unit is taken out of operation for defrost. This infers that the remaining 19 units have to supply the additional load. However, the evaporation temperature slowly recovers as the defrosted unit has a higher performance.

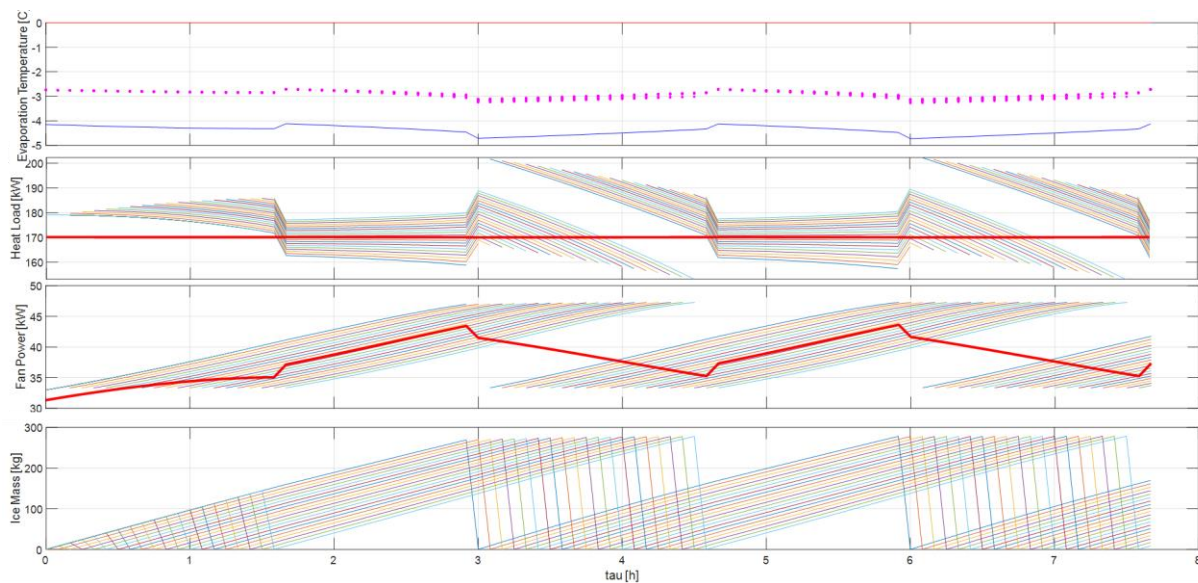


Figure 11. Operation of all 20 evaporator units with individual defrost every 3rd hours

Concluding points for the frost formation and defrost modelling

- A detailed temporally and spatially distributed model of an evaporator unit was developed
- A model of a complete evaporator field with frost formation and defrosting was developed
- Spatial distribution of frost accumulation and subsequent refrigerant and air mass distribution had a minor effect on the overall performance
- The main source of the performance degradation due to frost accumulation was the increased air flow resistance not the thermal resistance of the accumulated frost
- Heat transfer performance can be maintained if fan speed can be increased enough to maintain the air flow

- The distribution of heat load and fan power between the individual units of the evaporator field was significant and the overall performance should be modeled based on the entire field and not based on a single unit

Task 2. CFD analysis of evaporator layouts and air recirculation

The objective of this task was to give guidelines on how to design evaporator fields, where the heat pump performance is affected as little as possible by recirculation effects of the air, and the cold air produced in the evaporators affects neighboring areas as little as possible. The work focused on the horizontal evaporator layout, as this is the layout of the Brædstrup heat pump and is the layout most often chosen for large-scale ambient air source heat pumps.

The CFD analysis was documented in the open access paper by Rogié et al. [1]. The following guidelines partly summarize the work presented in the paper and draws some general conclusions from the work.

Guidelines to prevent air recirculation of an air-source large-scale heat pump

The following guidelines were developed based on the CFD studies that were carried out in Task 2. The guidelines provide concise recommendations, for more details on the CFD results and CFD modelling details we refer to Rogié et al. [1].

Air recirculation in a large-scale air-source heat pump occurs when a fraction of the cold air leaving the outlets of the heat pump evaporators recirculates back to the evaporator fan inlets. This leads to a lower mean inlet temperature, compared with the ambient temperature, and consequently to a lower coefficient of performance (COP) of the heat pump.

The recirculation is the consequence of large turbulent vortices created alongside the evaporators lateral edges (in the flow direction) due to the sudden change of wind trajectory. The higher the wind velocity, the stronger the vortices due to magnified kinetic energy dissipation, and therefore leading to higher recirculation. A view of the turbulent vortices around evaporators can be seen in Figure 7.

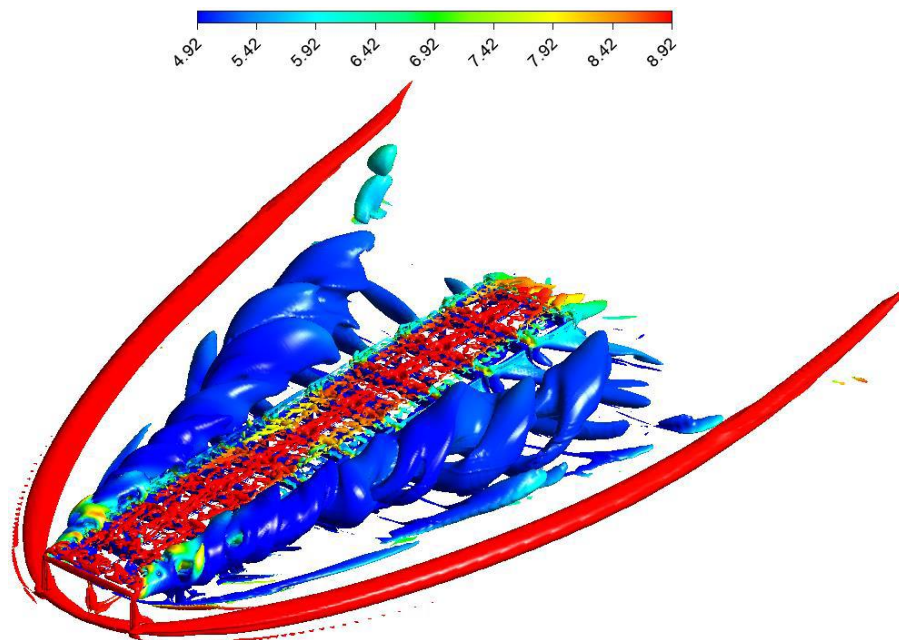


Figure 7: Turbulent vortex region of the flow around the evaporators

In order to prevent recirculation, two methods can be applied: (a) passive method and (b) active method.

a) The passive method consists of lowering the recirculation by placing the evaporators in an environment with a reduced incoming wind velocity. This can be done by having the evaporators in the wake of industrial buildings, taking advantages of natural obstacles (hill, large trees ...) or changing the layout of the evaporators.

However, certain care should be taken when placing the evaporators close to other large obstacles. In the example of evaporators placed in the wake of a sole building (evaporators downstream of building), the turbulent vortices created in wake of the building might increase the recirculation due to the chaotic flow motion at the leading edge of the evaporators. On the other hand, natural obstacles, such as a forest, might “absorb” the kinetic energy of the wind and decrease the incoming wind velocity at the evaporators, without creating upstream turbulent vortices. Therefore, one should be cautious with the use of obstacles to reduce the wind velocity, especially about the nature of the obstacles, their sizes, their numbers, and so on.

Concerning the evaporator layout, the fans impacted by the recirculation are generally located on the lateral sides of the evaporators (in regards to the wind direction) where the turbulent vortices are generated, as seen in Figure 7. In the case where no obstacles are present nearby the evaporators to decrease the wind velocity, the evaporators should be placed in order to limit the number of fans located on the lateral sides. Figure 8 represents the evolution of the recirculation rate depending on the wind direction.

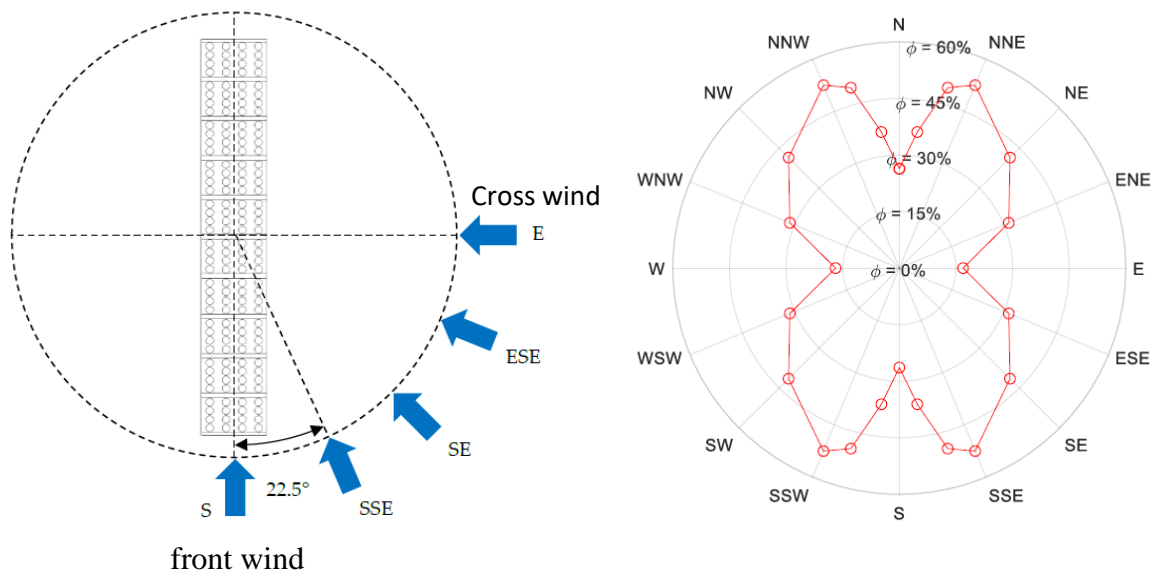


Figure 8: Recirculation ratio in function of the wind direction

It can be seen that the cross-wind configuration leads to the minimum recirculation ratio due to a lower number of fans located of the lateral edges (8 for cross-wind and 80 for front wind)

b) The active method consists of installing additional systems that will alter the flow motion out of the evaporator outlets, to avoid recirculation. One example is shown in Figure 9, where walls have been placed below the evaporators. These walls block the flow recirculating back to the fan inlets.

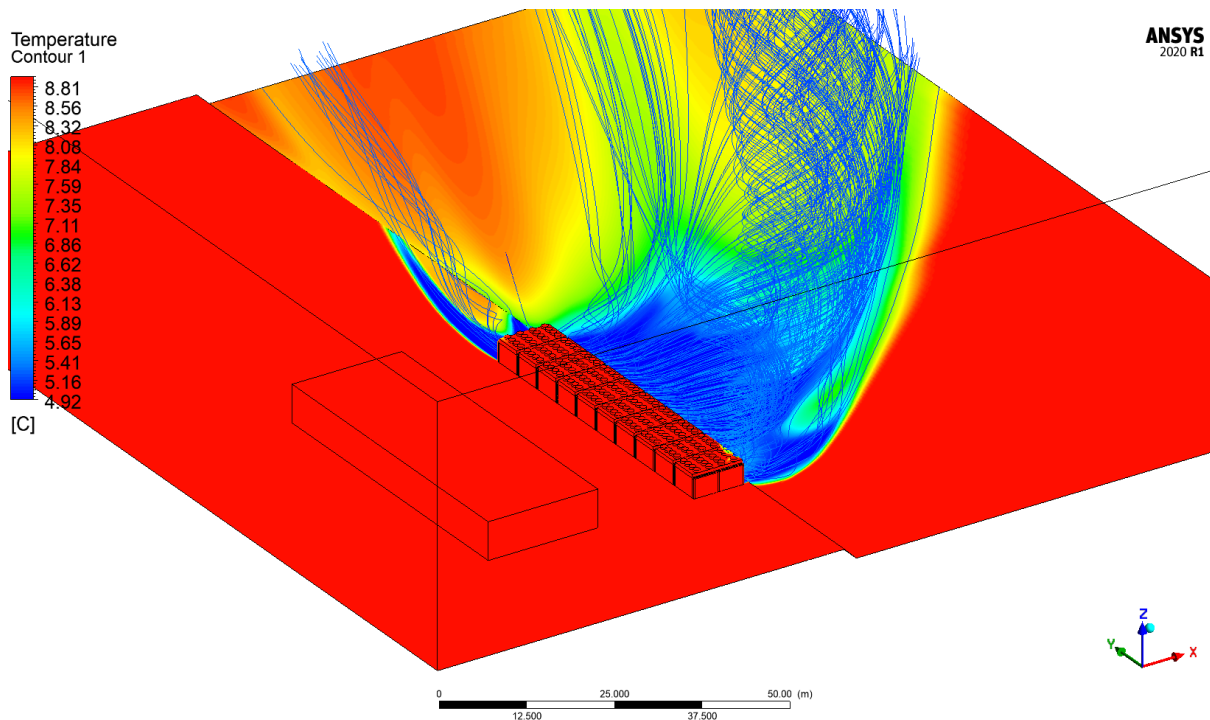


Figure 9: Flow motion around the evaporators with wind covers

It can be seen that the air is blocked at the lateral edges, which decreases the recirculation close to zero. In order to accommodate a change in the wind direction, flexible walls such as semi-rigid curtains, could be used instead of solid walls. The curtains should be able to open or close depending on the wind direction, to always ensure that the outlet cold air is blocked from recirculating along the turbulent vortices.

However, as opposed to the passive method, this system entrains an investment, operating and maintenance cost, as well as possible system failures due to its complexity.

Concluding points based on the CFD study

- Recirculation is caused by turbulent vortices on the side of the evaporators,
- Decreasing the wind velocity decreases the recirculation,
- Placing the evaporators behind obstacles, such as buildings, might reduce recirculation, at the condition that the flow is not too much disturbed by these obstacles,
- The use of natural obstacles, such as a forest, could possibly reduce recirculation without introducing flow disturbances,
- Placing the evaporators where strong wind is frequent (such as on top of a hill) should be avoided,
- Having wind covers below the evaporators decreases the recirculation to zero if they are placed facing the incoming wind.

References

- [1] W. . Rogié, B., Jensen, J.K, Hansen, S. O. K., & Markussen, “Analysis of Cold Air Recirculation in the Evaporators of Large-Scale Air-Source Heat Pumps Using CFD Simulations,” *Fluids*, vol. 5, no. 186, 2020.
- [2] M. Daminato, “Optimization of Evaporator Defrost Control for Large-Scale Air Source Heat Pumps,” DTU, 2021.
- [3] J. Kærn, M. R., Markussen, W. B., & Kristófersson, “Numerical analysis of flow maldistribution in large-scale liquid overfed finned-tube ammonia evaporators,” in *the 14th IIR-Gustav Lorentzen Conference on Natural Refrigerants*, 2020, pp. 251–256.
- [4] M. R. Kærn, “Analysis of flow maldistribution in fin-and-tube evaporators for residential air-conditioning systems,” DTU, 2011.
- [5] “MatLAB, version: 2018a, publisher: Mathworks.” Mathworks, Natick, Massachusetts, 2018.
- [6] E. W. Lemmon, M. L. Huber, and M. O. McLinden, “NIST standard reference database 23: reference fluid thermodynamic and transport properties (REFPROP), version 9.1, National Institute of Standards and Technology, Standard reference data program.” 2010.
- [7] N. H. KIM, J. H. YUN, and R. L. WEBB, “Heat transfer and friction correlations for wavy plate fin-and-tube heat exchanger,” *J. Heat Transf.*, vol. 119, no. 3, 1997.
- [8] S. Kaminski and U. Gross, “Luftseitiger Wärmeübergang und Druckverlust in Lamellenrohr-Wärmeübertragern,” *Luft-und Kältetechnik*, vol. 36, pp. 13–18, 2000.
- [9] V. Gnielinski, “New equations for heat and mass transfer in turbulent pipe and channel flow,” *Int. Chem. Eng.*, vol. 16, pp. 359–368, 1976.
- [10] H. Blasius, “Das Aehnlichkeitsgesetz bei Reibungsvorgängen in Flüssigkeiten,” *Mitteilungen über Forschungsarbeiten auf dem Gebiete des Ingenieurwes.*, vol. 134, 1913.
- [11] H. Ito, “Pressure Losses in Smooth Pipe Bends,” *J. Basic Eng.*, vol. 82, no. 1, pp. 131–143, 1960.
- [12] Q. S. Kelly, John E; Eckels, Steve J; Fenton, Donald F; Lies, “A survey of in-tube evaporation of ammonia heat transfer and pressure drop investigations,” *ASHRAE Trans.*, vol. 105, no. 110, 1999.
- [13] H. Müller-Steinhagen and K. Heck, “A simple friction pressure drop correlation for two-phase flow in pipes.”
- [14] D. F. Geary, “Return Bend Drop in Refrigeration Systems,” *ASHRAE Trans.*, vol. 81, pp. 250–265, 1975.
- [15] S. M. Zivi, “Estimation of steady-state steam void fraction by means of the principle of minimum entropy production,” *Trans. Am. Soc. Mech. Engrs, Ser. C, J. Heat Transf.*, vol. 86, pp. 247–252, 1964.